Determination of electrostatic potentials at biological interfaces using electron–electron double resonance

Yeon-Kyun Shin and Wayne L. Hubbell
Jules Stein Eye Institute and Department of Chemistry and Biochemistry, University of California, Los Angeles, California 90024-7008

ABSTRACT A new general method for the determination of electrostatic potentials at biological surfaces is presented. The approach is based on measurement of the collision frequency of a charged nitroxide in solution with a nitroxide fixed to the surface at the point of interest. The collision frequency is determined with ^{14}N: ^{15}N double label electron–electron double resonance (ELDOR). As a test, the method is shown to give values for phospholipid bilayer surface potentials consistent with the Gouy-Chapman theory, a simple model shown by many independent tests to accurately describe charged, planar surfaces. In addition, the method is applied to determine the electrostatic potential near the surface of DNA. The results indicate that the potential is significantly smaller than that predicted from Poisson-Boltzmann analysis, but is in qualitative agreement with that predicted by Manning's theory of counter ion condensation. The method is readily extended to measurement of surface potentials of proteins.

INTRODUCTION

The electrostatic potential at biological interfaces and macromolecular surfaces apparently plays a functional role in a number of interesting cases. The direct role of electrostatics in membrane phenomena is perhaps the most extensively investigated (for review, see McLaughlin, 1977; 1989). Biological membranes typically have a net negative charge, and the potential at the surface determines the local concentration of charged substrates for membrane-bound enzymes and transporters, determines to a large extent the repulsive forces between membranes, and may play a role in the determination of transmembrane lipid asymmetry (Hubbell, 1990). In addition, the interaction energies of charged peptides and proteins with membrane surfaces have a significant electrostatic component.

Electrostatic interactions also play interesting roles in the function of soluble proteins. For example, in superoxide dismutase, the electrostatic potential at the protein surface apparently serves to bias the diffusion of the charged substrate toward the active site, thus, increasing the effective catalytic rate constant (Sharp et al., 1987). Electrostatic interactions clearly play a role in protein–protein associations, as illustrated by the binding of cytochromes *b5* and *c* (Salemme, 1976; Rogers et al., 1988).

DNA-binding proteins have a significant electrostatic component to the binding energy. For example, in the "zinc finger" motif, a positively charged domain interacts directly with the DNA negative surface potential (for review see Kaptain, 1991).

Characterization of the energetics of interactions of the types mentioned above requires information on surface electrostatic potentials. In this paper, we describe a new general approach that can be used to obtain surface electrostatic potentials in any region of any system to which a nitroxide can be attached. In this approach, the attached nitroxide is used to probe the local concentration of a freely-diffusing, charged nitroxide in the aqueous phase through measurement of Heisenberg exchange by ELDOR spectroscopy. The local electrostatic potential is then determined from this concentration and the Boltzmann distribution of the charged nitroxide. In the case of phospholipid bilayers, the surface-associated probe nitroxide can be hydrophobically adsorbed or attached to the headgroup of a phospholipid (Kornberg and McConnell, 1971). In the case of proteins, the probe can be attached to a specific site using site-directed spin labeling (Altenbach et al., 1989; Todd et al., 1989). For nucleic acids, the nitroxide can be introduced either by covalent reaction or by intercalation (Bobst, 1979).

MATERIALS AND METHODS

Materials

Egg phosphatidylcholine (egg PC), 1-palmitoyl-2-oleoyl-phosphatidylglycerol (POPG), and 1-palmitoyl-2-oleoylphosphatidylcholine (POPC) were purchased from Avanti Polar Lipids, Inc. (Birmingham, AL). ^{14}N-tempol and ^{14}N-tempamine were obtained from Molecular Probes, Inc. (Eugene, OR). ^{15}N nitroxides were all purchased from MSD Isotopes Inc. (St. Louis, MO). Calf-thymus DNA was obtained from Sigma Chemical Co. (St. Louis, MO). 4-Morpholinopropanesulfonic acid (MOPS) was obtained from Research Organics, Inc. (Cleveland, OH).

0006-3495/92/06/1443/11 $2.00

N-(*N*-tempoyl)-palmitamide was prepared by the reaction of ^{15}N-tempamine with palmitoylchloride according to the following procedure. To a solution of tempamine (0.35 mM) and triethylamine (0.4 mM) in 2 ml of dry ether at 0°C was added dropwise with stirring over the course of an hour a solution of palmitoylchloride (0.30 mM) in ~1 ml of ether. The mixture was allowed to warm to room temperature and stand for 2–3 h and the triethylamine hydrochloride removed by filtration. The filtrate was diluted with ether to ~50 ml and washed five times each with 100 ml of water. The ether layer was dried with anhydrous sodium sulfate and the solvent removed under vacuum to yield an orange solid. The material was judged pure by thin layer chromatography on silica gel eluting with chloroform:methanol, 9:1 (*v*/*v*).

The spin label 9-tempaminoacridine was a gift of Dr. W. Struve. The synthesis is described by Sinha et al. (1976).

Sample preparation

To prepare lipid samples for surface potential measurement, chloroform stock solutions of egg PC and POPG were mixed in appropriate proportion to give 9.2 mol % negatively charged POPG in egg PC. A chloroform solution of *N*-(^{15}N-tempoyl) palmitamide was also added to give a ratio of spin label to phospholipid of ~ 0.01. The solution was then dried under nitrogen flow and subsequently under vacuum. An appropriate amount of 20 mM MOPS buffer of pH = 7.0 was then added to give a final concentration of ~ 25 mg/ml of lipid. The suspension was mixed on a vortex mixer and freeze-thawed five times. Unilamellar vesicles were prepared by passing the freeze-thawed lipid solution through 0.1 μm polycarbonate filters in an Extruder (Lipex Biomembranes Inc., Vancouver, BC, Canada). Small portions of ^{14}N-tempol and ^{14}N-tempamine stock solutions (10 mM) were then added to two separate aliquots taken from the above prepared vesicles. The concentrations of water soluble spin labels were ~1 mM. The ionic strength was adjusted with the permeable electrolyte ammonium acetate (Sundberg and Hubbell, 1986). Use of this electrolyte insured equal screening of both internal and external surfaces of the vesicles.

DNA samples were prepared by dissolving calf-thymus DNA in MOPS buffer (20 mM, pH = 7.2) of the desired ionic strength (determined by NaCl). In some experiments, 5 mM EDTA was included in the buffer to chelate divalent metal ions present in the DNA sample. The concentration of DNA phosphate was ~15 mM. An ethanol stock solution of 9-tempaminoacridine (100 mM) was added to achieve a ratio of acridine to phosphate of ~1/25.

ELDOR measurements

The ELDOR spectrometer is based on a 2-loop-1-gap resonator (Hubbell et al., 1987), and is of the same general design as that of Hyde et al. (1985), but includes a low-noise microwave preamplifier before the detector and an automatic frequency lock arm on the pump klystron. Details of the instrument will be published elsewhere. ELDOR reduction factors at infinite pumping power were determined as previously described (Hyde et al., 1968; Hyde and Feix, 1989). The excellent review by Hyde and Feix (1989) should be consulted for general information and definitions of the ELDOR terminology. In the present work, reduction factors were determined with a 100 KHz modulation frequency and an incident observe power of 0.2–0.4 mW. Reducing the modulation frequency to 25 KHz and/or the observe power by a factor of 3 had no effect on the observed reduction factors. Removal of oxygen was achieved by using a TPX sample tube and passing high purity nitrogen through the resonator assembly (Hyde and Subczynski, 1989). All experiments were performed at room temperature (20 ± 1°C).

THEORY

If there exists an electrostatic potential $\Psi(r)$ in solution, mobile ions are distributed in space according to Boltzmann statistics. The concentration $C(r)$ of an ion of charge Z at position r is given by

$$C(r) = C_0 \exp\left(-\frac{Z\mathcal{F}\Psi(r)}{RT}\right), \quad (1)$$

where C_0 is the concentration of the ion in the bulk phase where Ψ is taken to be zero, R is the gas constant, and $\mathcal{F}$ is the Faraday constant. Thus, if the ratio $C(r)/C_0$ of an ion at r is known, the electrostatic potential $\Psi(r)$ can be determined from Eq. 1. In the present experiments, we employ Heisenberg spin exchange to determine this ratio.

Heisenberg spin exchange is a process in which the members of a colliding radical pair exchange electronic spin states, and the spin exchange rate is proportional to the collision rate (Currin, 1962; Freed, 1966; Johnson, 1967; Eastman et al., 1969). An exchange event occurring between radicals with different nitrogen nuclear spin states produces observable spectral effects which may be used to deduce the collision rate and hence the local concentration of the colliding radical.

To use Heisenberg spin exchange to determine surface electrostatic potentials, one type of nitroxide group is fixed to the surface in the region of interest. This fixed group will be referred to as *F*, and serves to sense the local concentration of a charged mobile probe radical, *M*, in solution. In practice, *M* and *F* will be selected to have different isotopes of nitrogen in the nitroxide group, and are distinct magnetic species. All subsequent equations reflect this fact. The Heisenberg spin exchange rate $W_{ex}^{M\to F}$ felt by the fixed spin label *F* due to the spin label *M* is

$$W_{ex}^{M\to F} = p \cdot g \cdot 4\pi d D C^M(r), \quad (2)$$

where $C^M(r)$ is the local concentration of spin label *M* at point *r*, *d* is the collision radius, *D* is the relative diffusion coefficient, *p* is the probability of effective exchange per collision, and *g* is a steric factor to account for the fact that the influx of the spin label *M* at the position of *F* is, in general, not spherically symmetric due to geometric features of the environment of *F*. Collisions of small nitroxides in aqueous phase are, in general, in the "strong exchange limit" and $p=1/2$ (Freed, 1966; Eastman et al., 1969).

If the spin label *M* is ionic with valence *Z*, Eq. 2 can be rewritten with the help of Eq. 1 as

$$W_{ex}^{M\to F} = p \cdot g \cdot 4\pi d D C_0^M \exp\left(-\frac{ZF\Psi(r)}{RT}\right). \quad (3)$$

Because either $W_{ex}^{M\to F}$ or $W_{ex}^{F\to M}$ may be used to compute the total exchange rate between unlike spins, the following condition must be hold:

$$C^F[W_{ex}^{M\to F}] = C_0^M[W_{ex}^{F\to M}], \tag{4}$$

where C^F is the analytical concentration of F and C_0^M is the bulk concentration of M in the system. Eq. 4 assumes that all mobile species M are equivalent with respect to exchange with F, i.e., that equilibration between the surface and bulk phases is fast compared to the electron spin lattice relaxation time (T_e), and that the excess of M in the double layer is a small fraction of the total M population. (For the lipid concentrations used here (25 mg/ml), the average distance between vesicle surfaces (d = 1,000 Å) is ≈600 Å, and the distance from the vesicle surface to the bulk phase can be taken to be ≈300 Å. For an ion with a diffusion coefficient of 2×10^{-5} cm^2/s, the time for diffusion from the surface to the bulk is ~75 ns, short compared to the spin lattice relaxation time of ~0.5 to 1 microseconds. For the longest Debye length used (25 Å), the excess population of cations in the double layer is <5% of the total cation population in the bulk phase.)

Combining Eqs. 3 and 4, we find

$$W_{ex}^{F\to M} = p \cdot g \cdot 4\pi dDC^F \exp\left[-\frac{ZF\Psi(r)}{RT}\right]. \tag{5}$$

The quantities $pg4\pi dDC_0^M$ and $pg4\pi dDC^F$ in Eqs. 3 and 5 are simply the spin exchange rates in the absence of electrical interactions, for example, when spin label M bears no net electrical charge (i.e., $Z = 0$). Denoting these quantities as $W_{ex}^{M\to F,0}$ and $W_{ex}^{F\to M,0}$, respectively, Eqs. 3 and 5 may each be rearranged to give the potential as

$$\Psi(r) = -\frac{RT}{ZF}\ln\frac{W_{ex}^{M\to F}}{W_{ex}^{M\to F,0}} = -\frac{RT}{ZF}\ln\frac{W_{ex}^{F\to M}}{W_{ex}^{F\to M,0}}. \tag{6}$$

To use Eq. 6 to estimate potentials, it is necessary to obtain $W_{ex}^{M\to F}$ or $W_{ex}^{F\to M}$ for a charged probe and $W_{ex}^{M\to F,0}$ or $W_{ex}^{F\to M,0}$ for an uncharged spin label of the same size, diffusion coefficient and g factor. As has been pointed out, g mainly depends on the environment of the fixed spin label F and should be the same for all mobile spin labels, M, of similar size.

The ^{14}N:^{15}N "dual-label" experiment in cw-ELDOR (Stetter et al., 1976; Popp and Hyde, 1982) provides an excellent way of measuring the various Heisenberg spin exchange rates indicated in Eq. 6. Experimental and theoretical details of cw-ELDOR and the dual-label experiment have been extensively discussed by Feix and Hyde in a recent review (1989). Here we discuss only the part of ELDOR relevant to the electrostatic potential measurement.

Suppose that an ^{15}N (or ^{14}N) spin label is fixed at a particular site in the system of interest, and the solution contains a freely diffusing ^{14}N (or ^{15}N) spin label. If one isotopic spin (the "pumped species") is irradiated with a high microwave power of resonant frequency, ν_p, the saturation will be transferred to the other isotopic spin (the "observed species") only through Heisenberg spin exchange. The reduction of the ESR line intensity of the observed species induced by this saturation transfer is monitored by a second low microwave power at a resonant frequency of the observed species, ν_o.

The ELDOR reduction factor, R, is defined by (Hyde et al., 1968)

$$R = 1 - \frac{I_p}{I_0}, \tag{7}$$

where I_p is the ESR line intensity at ν_o with the pump power on and I_0 is the ESR line intensity with the pump power off. In the fast motional regime, the inverse of R is linearly proportional to the inverse of the pump microwave power. Extrapolation of a plot of R^{-1} vs P^{-1} to infinite pump power gives the quantity R_∞^{-1}, which is related to the exchange frequency. If all hyperfine states are strongly coupled (Yin and Hyde, 1987),

$$R_\infty^{-1} = \frac{2W_e}{W_{ex}} + 1, \tag{8}$$

where W_e is the spin-lattice relaxation rate ($=2/T_e$) of the observed spin label. The assumption of strongly coupled hyperfine states will be discussed below. From Eqs. 6 and 8 we obtain

$$\Psi(r) = \frac{RT}{ZF}\ln\frac{(R_\infty^{M\to F})^{-1} - 1}{(R_\infty^{M\to F,0})^{-1} - 1}\cdot\frac{C_0}{C_0^0}, \tag{9}$$

for the electrostatic potential $\Psi(r)$ when the freely diffusing spin label is pumped, and the fixed spin label F is observed. C_0^0 and C_0 are the bulk concentrations of the neutral and charged species, respectively. $R_\infty^{M\to F}$ and $R_\infty^{M\to F,0}$ are the extrapolated reduction factors of F due to collision with charged and neutral M, respectively.

Because we observe the common spin label F independent of the mobile species, W_e does not appear in Eq. 9. The ratio C_0/C_0^0 may be conveniently determined from the relative ratios of ESR intensity of these spin labels to that of the common fixed spin label F.

On the other hand, when the free spin label M is observed while pumping the fixed spin label F, the electrostatic potential $\Psi(r)$ is obtained from the equation

$$\Psi(r) = -\frac{RT}{ZF}\ln\frac{(R_\infty^{F\to M,0})^{-1} - 1}{(R_\infty^{F\to M})^{-1} - 1}\cdot\frac{W_e}{W_e^0}. \tag{10}$$

Here, it is assumed that the concentration of the fixed spin label C^F is kept constant for two samples. In this case, the ratio of the spin lattice relaxation rates W_e/W_e^0 for the charged to the neutral spin label probes must be known. This can be obtained from separate spin-lattice relaxation time measurements (Popp and Hyde, 1982).

In the present cw-ELDOR experiments, tempol (I), tempamine (II) and 3-carboxy-proxyl (III) have been used as neutral, cationic and anionic probe radicals, respectively. The structures are shown below.

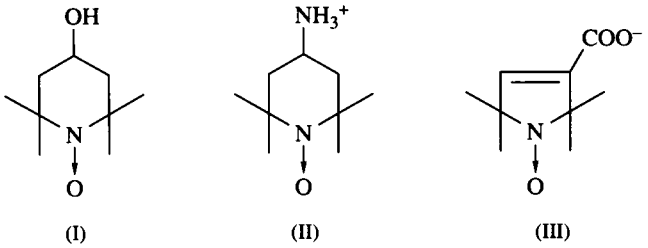

(I) (II) (III)

The fixed label is selected according to the specific application, as illustrated below.

RESULTS

Determination of membrane surface potentials

To investigate electrostatic potentials at membrane surfaces, a spin label must be introduced at the membrane/aqueous interface. In the above notation, this is the "fixed" spin label *F*. In the present experiments, *N*-(15*N*-tempoyl)-palmitamide, (IV) below, has been employed for this purpose.

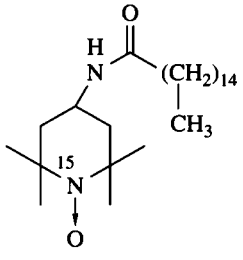

(IV)

This amphiphilic label binds strongly to membranes by virtue of its long hydrocarbon chain, but the polarity of the amide linkage is expected to localize the nitroxide function in the aqueous phase adjacent to the membrane surface. This location is confirmed by the isotropic hyperfine coupling of the bound species (23.8 G) and the accessibility of the nitroxide to collision with charged species (see below).

Fig. 1 shows the EPR spectrum of spin label (IV) bound to phospholipid vesicles in a solution containing ^{14}N-tempol. The ^{15}N and ^{14}N resonance lines are well resolved in the motionally narrowed spectra. The dotted line is the spectrum recorded with the pump power off and the solid line that with 30 mW of pump power. The ELDOR effect is clearly seen in the expected regions of the spectrum, indicating Heisenberg exchange between the two spin populations.

The method described here uses the ELDOR reduction of the fixed nitroxide to determine the local concentration of the mobile species. Eqs. 2 and 8 can be combined to give the relationship between these quantities as

$$[(R_\infty^{M\to F})^{-1} - 1]^{-1} = \frac{pg4\pi dDC^M}{2W_e}. \qquad (11)$$

This fundamental relationship was tested by determining R_∞^{-1} for spin label (IV) at POPC vesicle surfaces as a function of the concentration of ^{14}N-tempol in solution. The results are shown in Fig. 2, and verify the relation over a wide concentration range and justify the use of Eq. 9 for determination of potentials at membrane surfaces.

Electrostatic potentials at the surface of charged phospholipid bilayers have been shown to be accurately given by the Gouy-Chapman theory in many independent tests (McLaughlin, 1977; 1989; Cafiso and Hubbell,

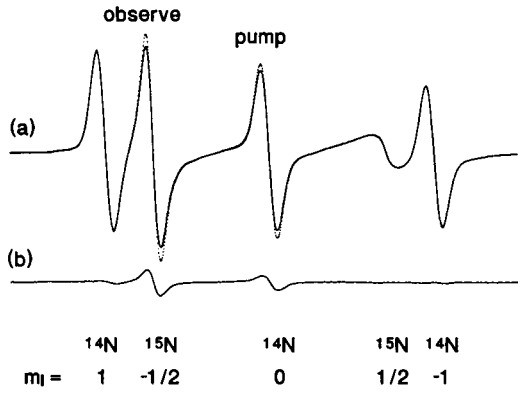

FIGURE 1 ESR and ELDOR spectra of spin label (IV) in egg PC/9.2 mol% POPG vesicles in the presence of ^{14}N-tempol in solution. (*a*) Superposition of ESR spectra with pump power off (*dotted line*) and with 30 mW incident pump power (*solid line*). The separation between observe and pump frequencies was $\nu_o - \nu_p = 33.5$ MHz, corresponding to the separation of the ESR transitions indicated. The ELDOR reduction can be seen at the "pump" and "observe" positions. (*b*) The ELDOR spectrum obtained by subtraction of the pump-on from the pump-off spectrum.

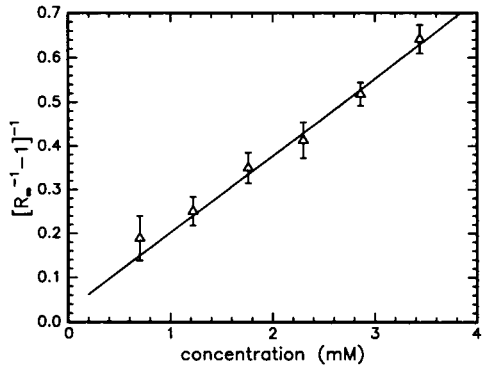

FIGURE 2 Plot of $[R_\infty^{-1} - 1]^{-1}$ for spin label (IV) in POPC vesicles vs concentration of ^{14}N-tempol in solution. The $M_I = 0$ ESR line of ^{14}N-tempol was pumped while the $M_I = -1$ ESR line of (IV) was observed.

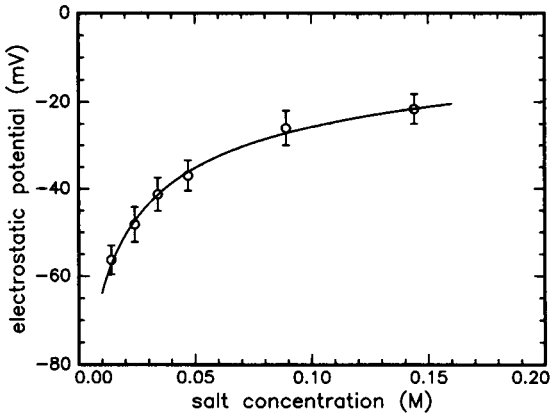

FIGURE 3 Plots of surface potential vs ionic strength for vesicles of egg PC/9.2 mol% POPG. The open circles are the experimentally determined values. The solid line is plotted according to the Gouy-Chapman theory including corrections for ion binding to POPG (see text). The error bars represent computed errors in the extrapolation to determine R_∞^{-1}. This is the dominant error in the measurement.

1978). Thus, this interface serves as an excellent test for the method.

Surface potentials were determined using the above method for unilamellar vesicles of egg PC with 9.2 mol % of POPG at various ionic strengths. The ELDOR reduction of (IV) was monitored while the center line ($M_I = 0$) of either ^{14}N-tempol or ^{14}N-tempamine was pumped ($\nu_o - \nu_p = 33.5$ MHz, cf Fig. 1). (As noted above, the charged and electrically neutral probe species must have similar diffusion coefficients and collision diameters. To verify this for the probes used, ELDOR experiments were performed for solutions containing: (1) ^{15}N-tempamine and ^{14}N-tempol; (2) ^{14}N-tempamine and ^{15}N-tempol; (3) ^{15}N-tempol and ^{14}N-tempol. When the common ^{15}N-tempol was observed in solutions (2) and (3) while pumping the ^{14}N species, the R_∞^{-1} values for ^{15}N-tempol were identical within experimental error. This indicates that the diffusion coefficients for tempol and tempamine are equal. Likewise, we obtain the same R_∞^{-1} when we pump the common ^{14}N-tempol while observing either tempamine or tempol in solutions (1) and (3). This indicates the spin-lattice relaxation rates for tempol and tempamine are also the same. Therefore, we can make use of Eqs. 9 and 10 to estimate the electrostatic potential without further corrections for the differences in dD and in W_e between the two spin labels.) The concentration of the mobile nitroxide was always kept below 3 mM at the surface of membrane. The results are shown as open circles in Fig. 3.

According to the Guoy-Chapman theory, the surface potential at a charged, planar interface is given by

$$\Psi = \frac{2RT}{ZF} \sinh^{-1}\left(\frac{136\sigma}{\sqrt{C}}\right), \qquad (12)$$

where σ is the charge density in charges per square angstrom and C is the molar concentration of 1:1 electrolyte.

In the experiments reported here, the solutions contain two species of cations, namely Na^+ ion from the MOPS buffer and PG molecules and NH_4^+ from ammonium acetate. Eisenberg et al. (1979) have shown that both Na^+ and NH_4^+ ions bind to PG and lower the effective charge density. If the association constants for 1:1 binding of Na^+ and NH_4^+ are K_1 and K_2, respectively, the effective equilibrium charge density is given by

$$\sigma = \frac{\sigma_o}{1 + (K_1[Na^+] + K_2[NH_4^+]) \exp\left(-\frac{ZF\Psi}{RT}\right)}, \qquad (13)$$

where σ_0 is the surface density of POPG molecules in the same units as the charge density. The solid line in Fig. 3 is plotted according to Eqs. 12 and 13 with $K_1 = 0.6\ M^{-1}$ and $K_2 = 0.17\ M^{-1}$, the values given by Eisenberg et al. (1979). The value for σ_o was computed from the known composition taking the area per lipid head group to be 70 Å^2 (Castle and Hubbell, 1976). As can be seen, the agreement between the measured values and the Gouy-Chapman prediction is excellent, with no adjustable parameters.

DNA surface potential

The ELDOR approach for estimating electrostatic potentials at surfaces is quite general and can be applied to any system for which a fixed nitroxide (F) can be provided. As shown above, that is readily accomplished for membranes. To demonstrate the generality of the

method, experiments were carried out to measure the electrostatic potential near the surface of the DNA duplex.

The 9-tempaminoacridine spin label (V) shown below has been shown to intercalate into the DNA double helix (Sinha and Chignall, 1975; Sinha et al., 1976; Bobst, 1979) and this has been used as the fixed spin label *F*.

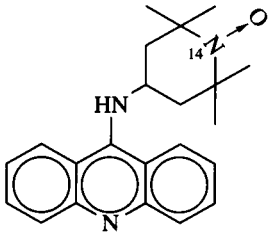

(V)

The structure of a complex with 9-aminoacridine intercalated into a miniature Watson-Crick double helix has been solved by crystallographic methods (Sakore et al., 1977). From these studies, it was concluded that the intercalative mode of 9-aminoacridine into DNA was a pseudo-symmetric association with the amino group pointing into the minor groove. Theoretical and experimental studies of intercalated 9-anilinoacridines support a structure in which the bulky 9-substituent is located in the minor groove (Denny et al., 1983; Abraham et al., 1988). Assuming that the 9-tempaminoacridine intercalates in a similar fashion, the nitroxide group would be located in the minor groove as shown in Fig. 4. If DNA is modeled as an extended cylinder of radius 10 Å, then the nitroxide group is expected to be near the cylindrical surface of the DNA strand.

The ESR spectrum of ^{14}N (V) bound to DNA is in the slow motional regime and has extensive overlap with the ^{15}N water soluble spin labels (cf Fig. 5 *a*). This is an unfavorable condition for performing the ELDOR experiment, because the pumped species contributes to the reduction in amplitude at the observe frequency. (Although the collision frequency between the bound ^{14}N-acridine labels is extremely low, ELDOR reduction is seen at all hyperfine lines of the species due to fast nuclear relaxation.) The problem may be overcome if the amplitude of the pumped (*F*) species can be made very small compared to the observed (*M*) species. This situation can be realized if the fixed ^{14}N (V) is pumped, because this species has a wide line width and low intensity relative to the mobile, deuterated, ^{15}N probe species (*M*). For example, in the composite spectrum of ^{15}N-tempol in solution and ^{14}N (V) intercalated into DNA, the intensity ratio at same concentration is at least 100:1 as can be seen in Fig. 5 *b*. Therefore, if the center line of the ^{14}N spectral component is pumped and the ^{15}N high intensity ESR line is observed, any ELDOR effects due to the ^{14}N spectral component can be neglected. (This approach was also used to obtain the surface electrostatic potential for egg PC/9.2 mol % POPG unilamellar vesicles using ^{14}N derivative of (I) and ^{15}N-deuterated tempol and tempamine. The surface potential obtained using Eq. 10 was the same as the results shown in Fig. 3 within experimental error.)

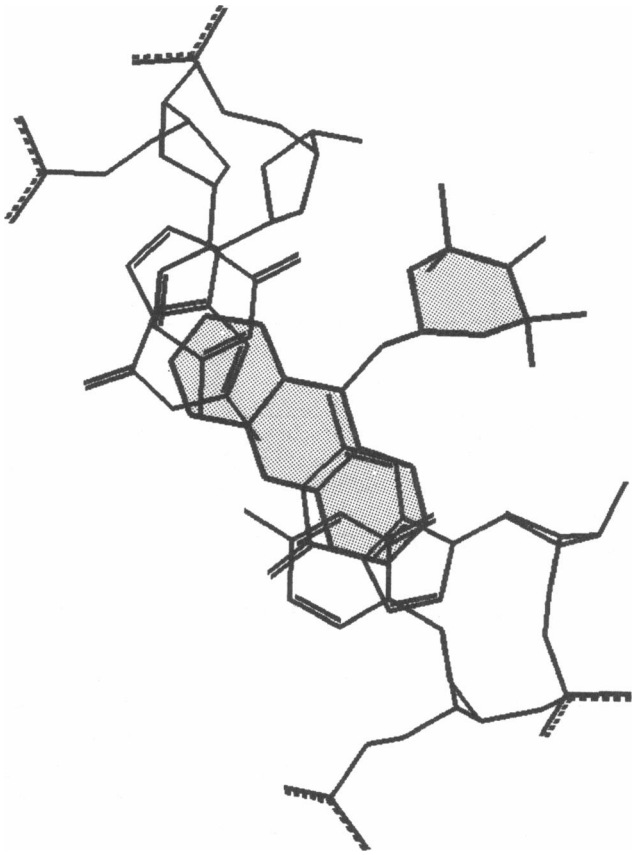

FIGURE 4 Molecular model of 9-tempaminoacridine intercalated in DNA. The view is down the base pairs, with the rings on the spin label shaded for identification. Only the base pairs at the intercalation site are shown. The nitroxyl ring points into the minor groove. The spin label position is schematic, and intended only to show the general location of the nitroxide ring in the groove.

To estimate the potential near the surface of DNA using (V) as the fixed label, ^{15}N-tempamine and ^{15}N-tempol were employed as the charged and neutral probe species, respectively, and ELDOR reductions interpreted in terms of Eq. 10. Results at several ionic strengths are illustrated by the open circles in Fig. 6. In principle, the potentials determined should be independent of the valence of the probe species. This was

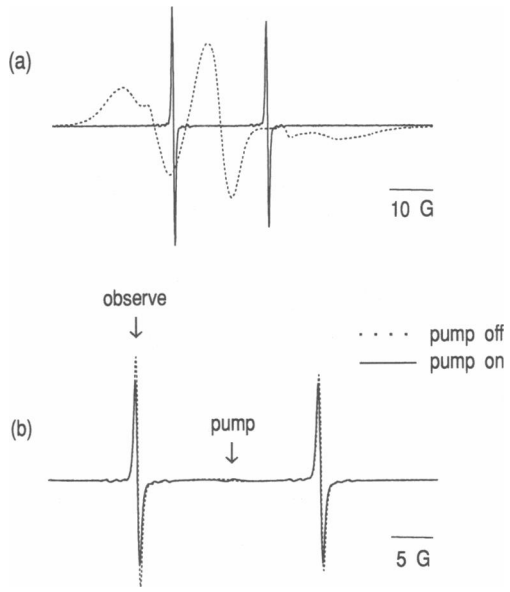

FIGURE 5 Composite ESR spectra of 9-tempaminoacridine (V) intercalated in DNA and ^{15}N-tempamine in solution. (*a*) ESR spectra of (V) intercalated in DNA and ^{15}N-tempamine in solution superimposed to illustrate spectral overlap. The relative gains are selected to display both line shapes with similar amplitudes. (*b*) ESR spectra of (V) intercalated in DNA and ^{15}N-tempamine in solution at identical concentrations (0.5 mM). The intensity of (V) is ~100 times less than that of the tempamine. The dashed line is with the pump off, and the solid line is with 30 mW of pump power and $\nu_o - \nu_p = 33.5$ MHz. Even though the intensity of (V) is too low to be seen, the effect of pumping this species is clearly detected at the ^{15}N positions. Note the difference in magnetic field scale between (*a*) and (*b*).

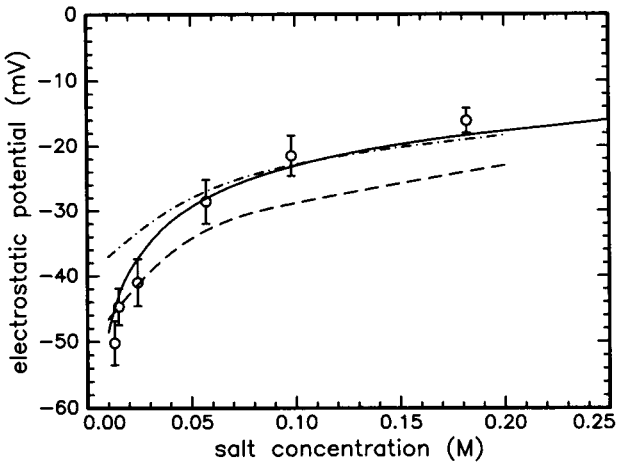

FIGURE 6 Plot of DNA surface potential vs ionic strength. Experimental results are shown as open circles. The theoretical results from nonlinearized Poisson-Boltzmann equation with reduced DNA phosphate charge of −0.2 (-·-) and −0.25 (---) are also shown. The solid line is the theoretical prediction from Eq. 15 with $\beta = 0.091$.

checked at 15 mM ionic strength using the anionic probe 2,2,5,5 tetramethylpyrroline-3-carboxy-^{15}N-oxyl (III). The result was the same as that from ^{15}N-tempamine with somewhat larger experimental error. This indicates that the cation probe does not show a significant direct ionic interaction with the phosphate backbone, an interaction which could lead to error in the estimation of potential. Inclusion of 5 mM EDTA in the buffer had no effect on the measured potentials.

The simplest theoretical model for the double helix is a uniformly charged cylinder with a linear charge density β. For low potentials, the analytic solution for the linearized Poisson-Boltzmann equation for this geometry is (Tanford, 1961),

$$\Psi(a) = \frac{2\beta}{\epsilon} \cdot \frac{K_0(\kappa a)}{(\kappa a)K_1(\kappa a)}, \qquad (14)$$

where K_0 and K_1 are the modified Bessel functions, ε is the dielectric constant of medium (ε = 80 for water), and κ is the Debye constant.

As shown by the solid line in Fig. 6, the experimental results obtained here for the DNA surface potential fit well with the simple cylindrical model expressed by Eq. 14, if the linear charge density is considerably reduced from the actual phosphate density. The best fitting value of β is 0.091 charge/Å, which corresponds to only 14% of the phosphate charge density. The significance of this will be discussed below.

DISCUSSION

The method presented above for the measurement of electrostatic potentials in surface phases is based on the assumption that mobile ions are distributed according to Boltzmann statistics and requires that the steric factors, diffusion constants and collision diameters of the charged and neutral probe species be the same. The probe molecules employed in this work are of very similar size and geometry, and it is reasonable to expect them to have similar diffusion constants and collision diameters. This was verified for tempol and tempamine, the primary charged/neutral pair employed.

The simple expression (8) for the reciprocal ELDOR reduction factor assumes strong coupling between the hyperfine states within both the ^{15}N and ^{14}N radical populations. For the fixed populations (*F*), rapid nitrogen nuclear relaxation insures this condition (Hyde et al., 1968). For the mobile solution radical (*M*), the correlation times are short and nuclear relaxation is not an efficient coupling mechanism. However, the concentration of the *M* radical is kept sufficiently high (≥0.5

mM) that self-exchange within the M population effectively couples the states. The linearity of the plot in Fig. 2 supports this conclusion.

The surface potential at a phospholipid bilayer has been so well characterized that it serves as an excellent test system for the technique. The data in Fig. 3 clearly illustrate that the ELDOR method quite accurately reports potentials consistent with Gouy-Chapman theory. Numerous experiments from many laboratories have established the validity of this theory for simple charged bilayer surfaces, and the results give credibility to the basis of the measurement.

A number of methods have been developed for the estimation of electrostatic potentials at biological interfaces, the majority of them directed at biological membranes. One class of such methods utilizes the potential-dependent partition coefficient of an amphiphilic ion to the membrane surface. Estimation of the partition coefficient has been determined, for example, by fluorescence (McLaughlin and Harary, 1976) or ESR (Castle and Hubbell, 1976), In general, this approach suffers two serious limitations. First, a zero-potential reference state is required to determine the hydrophobic contribution to the partition coefficient. In model systems, this is simple to achieve by simply omitting the charged component from the membrane, but for native membranes this of course cannot be done. The use of high salt concentration to reduce the potential to near zero is unsatisfactory, because extremely high ionic strengths must be used and this could cause reorganization of the membrane structure. An uncharged analogue of the amphiphilic ion cannot be used to estimate the hydrophobic contribution because it is likely that the charged and neutral species will occupy different positions in the bilayer. In some cases, the iso-electric point of the surface can be used as a zero potential reference, but it must be demonstrated that the charge distribution in this state is homogeneous (Tsui et al., 1990). The second difficulty with these methods is that potential changes are inferred directly from changes in partition coefficient of the amphiphilic ion. Unfortunately, partition coefficient changes can also occur due to structural changes in the membrane unrelated to potential.

The ELDOR method presented here is free from the above limitations. A zero electrical energy reference is required to determine the quantity $pg4\pi dD$ (see Eqs. 3 and 5), but this can be determined with either a neutral probe species of the same size and diffusion constant as the charged probe ($Z = 0$) or from an electrically neutral surface ($\Psi = 0$). Clearly, it is advantageous to choose the former for the reasons discussed above, and that has been done in the present work. Unlike partitioning methods, potential changes can be sensed directly in the ELDOR method through changes in collision frequency without complications arising from structural changes in the system. Such changes could effect the quantity $pg4\pi dD$, but this is automatically compensated by the reference measurement with the neutral probe species.

Heisenberg spin exchange is a short-range interaction, i.e., spin pairs exchange only under collision. For the small nitroxide probes used here, the collision radius is on the order of 4 Å, which is about the size of the nitroxide molecule (Hyde and Feix, 1989). This implies that the spatial resolution of the method is ~ 4 Å.

For measurement of membrane surface potentials, physical adsorption of a species like (IV) above provide a surface probe that will report the average "smeared" potential. Unlike partitioning approaches, the ELDOR method can also be used to determine potentials at heterogeneous solid surfaces such as the solvent/protein or solvent/nucleic acid interface. It has recently been demonstrated that nitroxide groups can be placed at virtually any chosen site on the surface of a protein with site-directed spin labeling (Altenbach et al., 1989; Todd et. al., 1989). Such specifically placed nitroxides serve admirably as fixed probes for the determination of local potentials. At heterogeneous solid surfaces such as those at proteins, potential gradients exist parallel to the surface, and these can be mapped by the placement of nitroxides at a number of different sites on the surface. Such experiments are currently underway (Y.-K. Shin, P. Stayton, S. Sligar, and W. L. Hubbell, unpublished results).

The determination of the potential near the surface of a DNA duplex illustrates the application of the method to this class of structures. The experimental value for the potential is of some interest because, to our knowledge, it has not been previously determined in a direct way. The experimental value for the electrostatic potential at the site of the nitroxide is considerably smaller than that predicted by numerical solutions of the nonlinear Poisson-Boltzmann equation for B-DNA, which is on the order of -150 mV at 25 mM monovalent salt concentration (Jayaram et al., 1989, 1990; Klement, 1991). Possible experimental errors that should be considered are: (*a*) direct binding of the positive probe molecule to the negative phosphates in the backbone, and (*b*) orientation of the charged probe but not the neutral probe in the intense field gradients at the surface. Both effects would make the apparent potential smaller in magnitude than the actual potential. Because both of these errors arise from the charge on the probe, they would reverse with a change in sign of the mobile probe. The fact that the same potential was determined with a negative as for a positive probe eliminates these errors as significant ones.

The intercalation of the acridine spin label (V) in

DNA causes local unwinding which is expected to reduce the charge density and electrostatic potential. This must account for at least some of the discrepancy. Detailed calculations based on the known structure of 9-aminoacridine in a miniature double-helix (Sakore et al., 1977) will be required to assess the importance of this factor in the Poisson-Boltzmann solution. This is beyond the scope of the present work.

Another possible explanation for experimental potentials lower than expected from the total charge density was offered by Manning (1969, 1978). His theory of "ion condensation" predicts that the charge density is reduced to ~20% of its maximum value for highly charged polyelectrolytes like DNA. Furthermore, the magnitude of this reduction is ionic strength independent once the counterion concentration exceeds that of the charge on the polyelectrolyte.

There is some experimental evidence in support of this theory. NMR investigations of Na^+ binding to DNA found that 75% of the phosphates on DNA were associated with Na^+, independent of the NaCl concentration (Anderson et al., 1978), consistent with the Manning theory. Other experiments based on dye binding (Wilson et al., 1985; Tanious et al., 1991) and electrophoresis (Armstrong et al., 1970) have also been interpreted in terms of the phenomenon of ion condensation.

To compare theoretical predictions of the ion condensation model with the data in Fig. 6, the electrostatic potential at the position of the nitroxide was computed using the program DELPHI (Biosym Technologies, Inc., San Diego, CA) with a reduced phosphate charge to simulate ion condensation. This program is a numerical solution to the nonlinear Poisson-Boltzmann equation. The results are shown as dashed lines in Fig. 6 for a phosphate charge of -0.2 and -0.25, the latter being the value predicted by Manning theory. The results are in qualitative agreement with the Manning model. However, the above calculation assumed that the presence of the intercalated spin label does not significantly alter the B-DNA potentials. This assumption must be checked before concluding that the results support the ion-condensation model.

As mentioned in Results, the solid line in Fig. 6 is the best fit to the data using the simple *linearized* Poisson-Boltzmann equation for a uniformly charged cylinder of radius 10 Å (Eq. 14). With the phosphate charge density reduced to 14% of its full value, this analytical expression fits the data extremely well. In principle, the expression is only valid for potentials $\ll |25|$ mV, and would not a priori be expected to fit the data well. However, Kotin and Nagasawa (1962) found similar results, and showed that the simple expression (Eq. 14) gives the same form as the complete nonlinear PB equation if a reduced effective charge is utilized. Even though the physical basis for this agreement is not entirely clear, Eq. 14 can be employed as a very useful empirical expression for computational purposes.

The above discussion has focussed on the utility of the collisional method for determination of local potentials. The general framework of the method may be developed using fluorescence as well as EPR spectroscopy. For example, Winiski et al. (1988) recently utilized the fluorescence quenching technique to measure the local electrostatic potential at some distance away from the membrane surface. The basic idea of the experiment is quite similar to that of the ELDOR experiment except that the neutral membrane is taken as the reference.

In ELDOR experiments the spin-lattice relaxation rate serves as the "clock" by which the saturation transfer rate is measured (cf Eq. 8). Thus, the Heisenberg spin exchange rate W_{ex} must be on the order of W_e to have a significant ELDOR effect, and the concentration of pumped species should be $\approx (2\pi dDT_{1e})^{-1}$. On the other hand, the fluorescence life time τ serves as the "clock" by which the quenching efficiency is measured in the fluorescence quenching experiment. Thus, the energy transfer rate ($=4\pi dDC$) must be on the order of $1/\tau$ to have detectable quenching efficiency, and the quencher concentration should be $\approx (4\pi dD\tau)^{-1}$. Because the nitroxide T_{1e} is typically on the order of a microsecond and the fluorescence life time for an organic fluorophore is typically on the order of 10 ns (Lakowicz, 1983), it is clear that a fluorescence quencher must be on the order of 100 times more concentrated than an ELDOR probe species.

On the other hand, excited lanthanide (e.g., terbium) complexes have a millisecond luminescence life time, and energy transfer from lanthanide complexes to chromophores in solution can be effective even at quite low probe concentrations (Wensel et al., 1985; Northrup et al., 1990). However, the energy transfer mechanism involves both collisional and dipolar components, and these must be separated for quantitative analysis. For surface situations where the steric factor g significantly reduces the collisional energy transfer rates, the energy-transfer mechanism is likely to be dominated by the dipolar contributions. In this circumstance, the energy transfer rate is a function of the spatial distribution of electrostatic potentials around the site of interest, and a local potential is not determined. For ^{14}N:^{15}N ELDOR in which one radical is in the liquid phase, Heisenberg spin exchange is the only significant saturation transfer mechanism and the data can be quantitatively analyzed in terms of the local electrostatic potential. This is considered to be a clear advantage of the ELDOR method.

We wish to thank Profs. James S. Hyde and Wojciech Froncisz for their invaluable assistance and encouragement in the design and construction of the University of California at Los Angeles ELDOR spectrometer.

This research was supported by National Institutes of Health Grant EY05216, a grant from Research to Prevent Blindness, and the Jules Stein Professor Endowment.

Received for publication 30 September 1991 and in final form 6 February 1992.

REFERENCES

Abraham, Z. H., M. Agbandje S. Neidle, and R. M. Acheson. 1988. Experimental DNA-binding and computer modelling studies on an analogue of the anti-tumor drug amsacrine. *J. Biomol. Struct. Dyn.* 6:471–488.

Anderson, C. F., M. T. Record, Jr, and P. A. Hart. 1978. Sodium-23 NMR studies of cation-DNA interactions. *Biophys. Chem.* 7:301–316.

Altenbach, C., S. L. Flitsch, H. G. Khorana, and W. L. Hubbell. 1989. Structural studies on transmembrane protein. 2. Spin labeling of bacteriorhodopsin mutants at unique Cysteine. *Biochemistry.* 28:7806–7812.

Armstrong, R. W., T. Kurucsev, and V. P. Strauss. 1970. The interaction between acridine dyes and deoxyribonucleic acid. *J. Am. Chem. Soc.* 92:3174–3181.

Bobst, A. M. 1979. Application of spin labeling to nucleic acids. *In* Spin Labeling II, Theory and Applications. L. J. Berliner, editor. Academic Press, Inc., New York. 291–345.

Cafiso, D. S., and W. L. Hubbell. 1978. Estimation of transmembrane potential from phase equilibria of hydrophobic paramagnetic ions. *Biochemistry.* 17:187–195.

Castle, J. D., and W. L. Hubbell. 1976. Estimation of membrane surface potential and charge density from the phase equilibria of a paramagnetic amphiphile. *Biochemistry.* 15:4818–4831.

Currin, J. D. 1962. Theory of exchange relaxation of hyperfine structure in electron spin resonance. *Phys. Rev.* 126:1995–2001.

Denny, W. A., G. J. Atwell, and B. C. Baguley. 1983. Potential antitumor agents. 39. Anilino ring geometry of amsacrine and derivatives: relationship mto DNA binding and antitumor activity. *J. Med. Chem.* 26:1625–1630.

Eastman, M. P., R. G. Kooser, M. R. Das, and J. H. Freed. 1969. Studies of Heisenberg spin exchange in ESR spectra. I. Linewidth and saturation effects. *J. Chem. Phys.* 51:2690–2709.

Eisenberg, M., T. Gresalfi, T. Riccio, and S. Mclaughlin. 1979. Adsorption of monovalent cations to bilayer membranes containing negative phospholipids. *Biochemistry.* 18:5213–5222.

Freed, J. H. 1966. On Heisenberg spin exchange in liquid. *J. Chem. Phys.* 45:3452–3453.

Hubbell, W. L., 1990. Transbilayer coupling mechanism for the formation of lipid asymmetry in biological membranes. Application to the photoreceptor disc membranes. *Biophys. J.* 57:99–108.

Hubbell, W. L., W. Froncisz, and J. S. Hyde. 1987. Continuous and stopped flow EPR spectrometer based on a loop-gap resonator. *Rev. Sci. Instrum.* 58:1879–1886.

Hyde, J. S., C. W. Chien, and J. H. Freed. 1968. Electron–electron double resonance of free radicals in solution. *J. Chem. Phys.* 48:4211–4226.

Hyde, J. S., and J. B. Feix. 1989. Electron–electron double resonance. *In* Biological Magnetic Resonance, Vol. 8. L. J. Berliner and J. Reuben, editors. Plenum Publishing Corp., New York. 305–337.

Hyde, J. S., and W. K. Subczynski. 1989. Spin-label oxymetry. *In* Biological Magnetic Resonance. Vol. 8. L. J. Berliner and J. Reuben, editors. Plenum Publishing Corp., New York. 399–425.

Hyde, J. S., J.-J. Yin, W. Froncisz, and J. B. Feix. 1985. Electron–electron double resonance (ELDOR) with a loop-gap resonator. *J. Magn. Res.* 63:142–150.

Jayaram, B., K. A. Sharp, and B. Honig. 1989. The electrostatic potential of B-DNA. *Biopolymers.* 28:975–993.

Jayaram, B., S. Swaminathan, D. L. Beveridge, K. A. Sharp, and B. Honig. 1990. Monte Carlo simulation studies on the structure of the counterion atmosphere of B-DNA. Variations on the primative dielectric model. *Macromolecules.* 23:3156–3165.

Johnson, C. S., Jr. 1967. Theory of line widths and shifts in electron spin resonance arising from spin exchange interactions. *Mol. Phys.* 12:25–31.

Kaptain, R. 1991. Zinc fingers. *Curr. Opin. Struct. Biol.* 1:63–69.

Klement, R., D. M. Soumpasis, and T. M. Jovin. 1991. Computation of ionic distributions around charged biomolecular structures: results for right handed and left handed DNA. *Proc. Natl. Acad. Sci. USA.* 88:4631–4635.

Kornberg, R. D., and H. M. McConnell. 1969. Inside-outside transition of phospholipids in vesicle membranes. *Biochemistry.* 10:1111–1120.

Kotin, L., and M. Nagasawa. 1962. Chain model for polyelectrolytes. VII. Potentiometric titration and ion binding in solutions of linear polyelectrolytes. *J. Chem. Phys.* 36:837–879.

Lakowicz, J. R. 1983. Principles of Fluorescence Spectroscopy. Plenum Publishing Corp., New York. 258–295.

Manning, G. S. 1969. Limiting laws and counterion condensation in polyelectrolyte solution. I. Colligative properties. *J. Chem. Phys.* 51:924–933.

Manning, G. S. 1978. The molecular theory of polyelectrolyte solutions with applications to the electrostatic properties of polynucleotides. *Quart. Rev. Biophys.* 2:179–246.

McLaughlin, S. 1977. Electrostatic potential at membrane-solution interfaces. *Curr. Top. Membr. Transp.* 9:71–144.

McLaughlin, S. 1989. The electrostatic properties of membranes. *Annu. Rev. Biophys. Biophys. Chem.* 18:113–136.

McLaughlin, S., and H. Harary. 1976. The hydrophobic adsorption of charged molecules to bilayer membranes: a test of the applicability of the Stern equation. *Biochemistry.* 15:1941–1948.

Northrup, S. H., T. G. Wensel, C. F. Meares, and J. J. Wendoloski. 1990. Electrostatic field around cytochrome *c*: theory and energy transfer experiment. *Proc. Natl. Acad. Sci. USA.* 87:9503–9507.

Popp, C. A., and J. S. Hyde. 1982. Electron–electron double resonance and saturation recovery studies of nitroxide electron and spin-lattice relaxation times and Heisenberg exchange rate: lateral diffusion in dimyristoyl phosphatidylcholine. *Proc. Natl. Acad. Sci. USA.* 79:2559–2563.

Rogers, K. K., T. C. Pochapsky, and S. G. Sligar. 1988. Probing the mechanisms of macromolecular recognition; the Cytochrome b_5-Cytochrome *c* complex. *Science (Wash. DC).* 240:1657–1659.

Sakore, T. D., S. C. Jain, C.-C. Tsai, and H. M. Sobell. 1977. Mutagen-nucleic acid intercalative binding: structure of a 9-aminoacridine:5-iodocytidylyl(3'-5')guanosine crystalline complex. *Proc. Natl. Sci. Acad. USA.* 74:188–192.

Salemme, F. R. 1976. An hypothetical structure for an intermolecular

electron transfer complex of Cytochrome *c* and b_5. *J. Mol. Biol.* 102:563–568.

Sharp, K., R. Fine, and B. Honig. 1987. Computer simulations of the diffusion of a substrate to an active site of an enzyme. *Science (Wash. DC).* 236:1460–1463.

Sinha, B. K., and C. F. Chignell. 1975. Acridine spin labels as probes for nucleic acids. *Life Sci.* 17:1829–1836.

Sinha, B. K., R. L. Cysyk, D. B. Millar, and C. F. Chignell. 1976. Synthesis and biological properties of some spin-labeled 9-aminoacridines. *J. Med. Chem.* 19:994–998.

Stetter, E., E.-H. Vieth, and K. H. Hausser. 1976. ELDOR studies of nitroxide radicals: discrimination between rotational and translational correlation times in liquids. *J. Magn. Res.* 23:493–504.

Sundberg, S. A., and W. L. Hubbell. 1986. Investigation of surface potential asymmetry in phospholipid vesicles by a spin label relaxation method. *Biophys. J.* 49:553–562.

Tanious, F. A., S.-F. Yen, and W. D. Wilson. 1991. Kinetics and equilibrium analysis of a threading intercalation mode; DNA sequence and ion effects. *Biochemistry.* 30:1813–1819.

Tanford, C. 1961. Physical Chemistry of Macromolecules. John Wiley and Sons, Inc., New York. 457–525.

Todd, A. P., J. Cong, F. Levinthal, C. Levinthal, and W. L. Hubbell. 1989. Site-directed mutagenesis of Colicin E1 provides specific attachment sites for spin labels whose spectra are sensitive to local conformation. *Proteins.* 6:294–305.

Tsui, F. C., S. A. Sunberg, and W. L. Hubbell. 1990. Distribution of charge on photoreceptor disc membranes and implications for charged lipid asymmetry. *Biophys. J.* 57:975–993.

Wensel, T. G., C.-H. Chang, and C. F. Meares. 1985. Diffusion-enhanced Lanthanide energy-transfer study of DNA-bound Cobalt (III) bleomycins: comparisons of accessibility and electrostatic potential with DNA complexes of ethidium and acridine orange. *Biochemistry.* 24:3060–3069.

Wilson, W. D., C. R. Krishnamoothy, Y. H. Wang, and J. C. Smith. 1985. Mechanism of intercalation: ion effects on the equilibrium and kinetic constants for the interaction of Propidium and Ethidium with DNA. *Biopolymers.* 24:1941–1961.

Winiski, A. P., M. Eisenberg, M. Langner, and S. McLaughlin. 1988. Fluorescence probes of electrostatic potential 1 nm from the membrane surface. *Biochemistry.* 27:386–392.

Yin, J.-J., and J. S. Hyde. 1987. Application of rate equations to ELDOR and saturation recovery experiments on ^{14}N:^{15}N spin label pairs. *J. Magn. Res.* 74:82–93.